THE JOURNAL OF PHYSICAL CHEMISTRY C

Article

pubs.acs.org/JPCC

Encapsulation of Au Nanoparticles on a Silicon Wafer During Thermal Oxidation

M. Bowker,*[,†,‡] J. J. Crouch,[†,∥] A. F. Carley,[†] P. R. Davies,[†] D. J. Morgan,[†] G. Lalev,[†,§] S. Dimov,[§,⊥] and D.-T. Pham[§,⊥]

[†]Wolfson Nanoscience Laboratory, School of Chemistry, Cardiff University, Cardiff CF10 3AT, United Kingdom

[‡]Rutherford Appleton Laboratory, Research Complex at Harwell (RCaH), Harwell, Oxon OX11 0F, United Kingdom

[§]Manufacturing Engineering Centre, Cardiff University, Queen's Buildings, The Parade, Newport Road, Cardiff CF24 3AA, United Kingdom

Supporting Information

ABSTRACT: We report the behavior of Au nanoparticles anchored onto a Si(111) substrate and the evolution of the combined structure with annealing and oxidation. Au nanoparticles, formed by annealing a Au film, appear to "float" upon a growing layer of SiO_2 during oxidation at high temperature, yet they also tend to become partially encapsulated by the growing silica layers. It is proposed that this occurs largely because of the differential growth rates of the silica layer on the silicon substrate between the particles and below the particles due to limited access of oxygen to the latter. This in turn is due to a combination of blockage of oxygen adsorption by the Au and limited oxygen diffusion under the gold. We think that such behavior is likely to be seen for other metal−semiconductor systems.

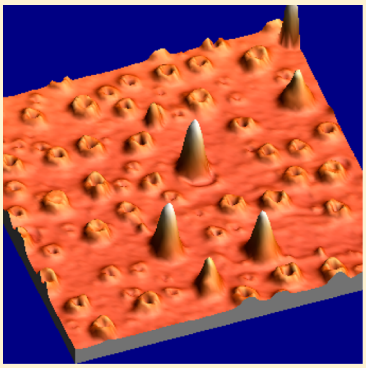

INTRODUCTION

Thin layers and nanoparticles of metals on semiconductor or oxide surfaces are of great importance in catalysis, semiconductor fabrication, sensors, and even in anticancer therapies and nanotoxicology. In catalysis, for instance, such nanoparticles are often the active phase in the reactions involved and gold, the subject of this paper, has become a focus of enormous interest in catalysis in the last 20 years or so. Although it was previously considered inert, Haruta[1,2] originally showed that nanogold supported on TiO_2 or Fe_2O_3 is the most active material for low-temperature CO oxidation, and it has recently been used for other important applications such as peroxide synthesis[3] and selective oxidation reactions.[4] Furthermore, a major problem in catalysis is the stability of nanoparticles, which is limited at elevated temperatures because of a variety of ripening processes.

However, the behavior of nanoparticles is perhaps of even greater importance for the huge technological area of semiconductor devices and their fabrication. In this area, the move over the last 30 years has been to compress more and more power into the semiconductor-based chips involved, and this is done by down-sizing the features well into the nano regime. The discrete nature of Au nanoparticles also attracts a lot of interest in the manufacturing of portable diagnostic devices based on local surface plasmon resonance (LSPR).[5,6] As in catalysis, the integrity of such fine structures is crucial to performance, and this integrity becomes more difficult to maintain as the features become even smaller because of the increased relative importance of atomic diffusion and hence loss of prefabricated structure. The work here relates to the integrity of structures at the nanoscale and in particular to the effect of thermal annealing in an oxidative environment on such integrity. We believe that understanding the effect of thermal treatment has important consequences for device manufacture and may represent an opportunity to stabilize such structures with respect to metal atom migration and sintering.

Previously we reported on the behavior of Au films and nanoparticles on single-crystal alumina[7,8] and showed that there was little evidence of sintering, the film behavior being dominated by dewetting above 400 °C and by thermal evaporation above 1000 °C. In this work we look at the effect of changing the substrate to single-crystal Si, and we report very different behavior, especially in terms of the effect of thermal treatment which results in partial encapsulation of Au nanoparticles on the single-crystal Si.

EXPERIMENTAL SECTION

Si(111) single-crystal of 5N purity was used as a substrate and was cleaned in the normal ways to produce a flat, particle-free surface with only a native oxide present. The deposition of a thin layer of Au onto the substrate was achieved by resistive evaporation: a sample of Au wire was placed in a tungsten

Received: July 25, 2013
Revised: September 20, 2013
Published: September 20, 2013

   dx.doi.org/10.1021/jp4074043 | J. Phys. Chem. C 2013, 117, 21577−21582

evaporation boat and mounted in a thermal resistive evaporator. The film thickness was monitored during the deposition process using a precalibrated crystal monitor, and the thickness of the film used here was 15 nm. Heating of these films was carried out in ambient air for two hours at various temperatures as described below.

A cross-beam focus ion beam (FIB) system (Carl Zeiss, 1540 XB) was employed for cross-sectional cuts and imaging. It comprises an ion beam column (OrseyPhysics) and a LEO Gemini SEM column. The system is equipped with a gas injection system (GIS) for local deposition or etching, an EDX detector for compositional analysis, an electron backscattering detector, scanning TEM detector, and Raith electron beam lithography software and hardware. This system also has the capability of real-time SEM observation during ion milling.

To study the morphology of the Au-SiO_2 film on Si, very fine FIB cross-sectional cuts were made utilizing a Ga ion beam at 30 kV and 50 pA. To protect the top film surface during the ion milling, Pt gas injection deposition was applied locally. In fact, there are two types of deposited Pt (see Figure 3 for instance). The first Pt layer is deposited by electron beam gas injection. This is a thin layer, typically 30−80 nm, which serves as a protective layer for the subsequent much thicker ion beam gas injection deposition in which Ga ions are likely to cause sputtering of the substrate. Usually, the electron-beam-deposited Pt appears darker (because of the increased C content) than the ion-beam-deposited layer.

SEM was employed for detailed observation of the evolution of the Au-SiO_2 film. Because of the film (electron) sensitivity and its poor conductivity, a low electron energy of 3 kV was applied. The unique SEM "in lens" detector provided an excellent (compositional and morphological) contrast, which further facilitated this investigation. All SEM images are taken at 36 degree tilt. For all measurements in the z direction, the tilt compensation option of the SmartSEM software was applied to obtain the correct measured values (e.g., the film depth).

AFM images were obtained using a Veeco Multimode with Nanoscope IIIa controller, with a contact mode tip, as the Si surfaces were hard enough to withstand the force exerted by this mode of operation. Image processing was carried out using the WSxM package.[9]

RESULTS AND DISCUSSSION

The gold was deposited by thermal evaporation onto a Si wafer, covering it to a thickness of ∼15 nm. X-ray photoelectron spectra (XPS) analysis of the Si wafer without Au showed the presence of the well-known native oxide layer[10] on the surface of the Si at ambient temperature. From the relative Si(IV):Si(0) ratio in XPS, and an inelastic mean free path of 3 nm[10] we can estimate the thickness of this layer[11] as ∼1 nm, in agreement with the literature.[12] This layer is little changed by heating to 500 °C for two hours in ambient air, but at higher temperature the oxidized layer begins to grow in thickness (this behavior can also be seen in Figure 1).

The XPS from the Au-coated, unheated sample is shown in Figure 1; the very weak Si(2p) signal is consistent with the presence of a thick layer of Au with few pinholes. Insignificant changes are observed with annealing up to 400 °C, but by 500 °C, the Au dewets from the silicon surface, as evidenced by the appearance of the Si signal in the XPS data and the AFM data shown below. Note that at this point the Si surface is still only partially oxidized and is similar to the native oxide layer. The spectrum changes after heating to 700 °C (Figure 1) with only

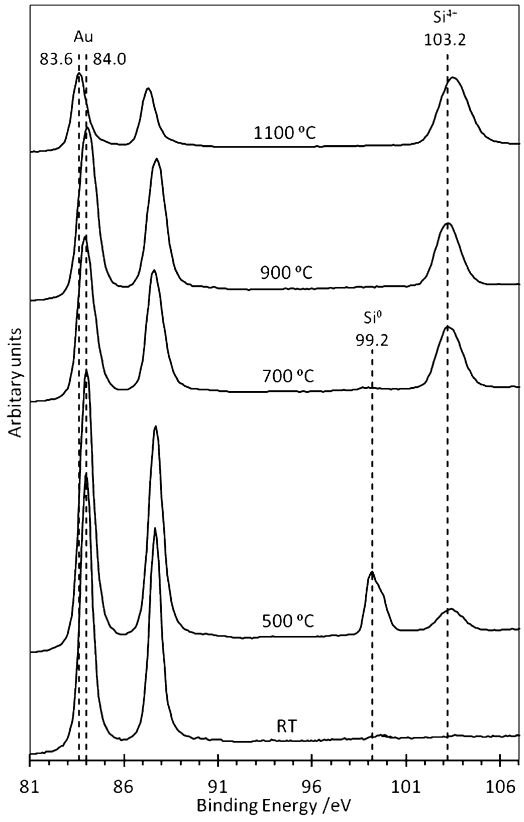

Figure 1. X-ray photoelectron spectra of the Au-coated silicon sample before and after the heating experiments, showing the Au(4f) and the Si(2p) regions. There is only a very small Si signal before heating to 400 °C, indicating near complete coverage of the Si sample by Au, but the substrate Si^0 signal appears at 500 °C, and is subsequently lost as it is oxidized at higher temperatures, forming a thick SiO_2 interface.

a small Si(0) peak remaining at 99 eV and a large peak at 103 eV for Si(IV), indicating an oxide thickness of ∼9 nm. By 900 °C, even this small Si(0) signal has disappeared because of further thickening of the silica layer; however, the Au:total Si peak height ratio is little changed, showing that minimal changes in the Au film have occurred compared with the sample annealed at 500 °C. However, large changes in this ratio are seen in Figure 1 after heating to 1100 °C, with a significant reduction in the relative Au signal. Resolving whether this is due to (i) loss of Au from the surface, (ii) sintering, or (iii) some other cause is aided by the AFM imaging presented below.

When gold is deposited, the AFM images show a smooth but polycrystalline film on the surface (see Figure 1 of the Supporting Information), and annealing the material to 400 °C has little effect on this surface layer. However, once heated to 500 °C, the Au film dewets from the surface of the Si and forms an array of nanoparticles. This layer is then reasonably stable, showing little evident change in particle size distribution, even up to 900 °C (Figure 2a), consistent with the minimal change in Au:Si ratio in the XPS. The particles in Figure 2a have an average size of ∼300 nm (see Figure 2 of the Supporting Information for the particle size distribution (PSD) analysis) and are relatively flat-topped (see Figure 3 of the Supporting Information for line profiles of the particles). However, dramatic changes occur after heating to 1100 °C, as shown in Figure 2b. At first glance, there appear to be far fewer particles in the wide scan image, and they are apparently much smaller

dx.doi.org/10.1021/jp4074043 | J. Phys. Chem. C 2013, 117, 21577−21582

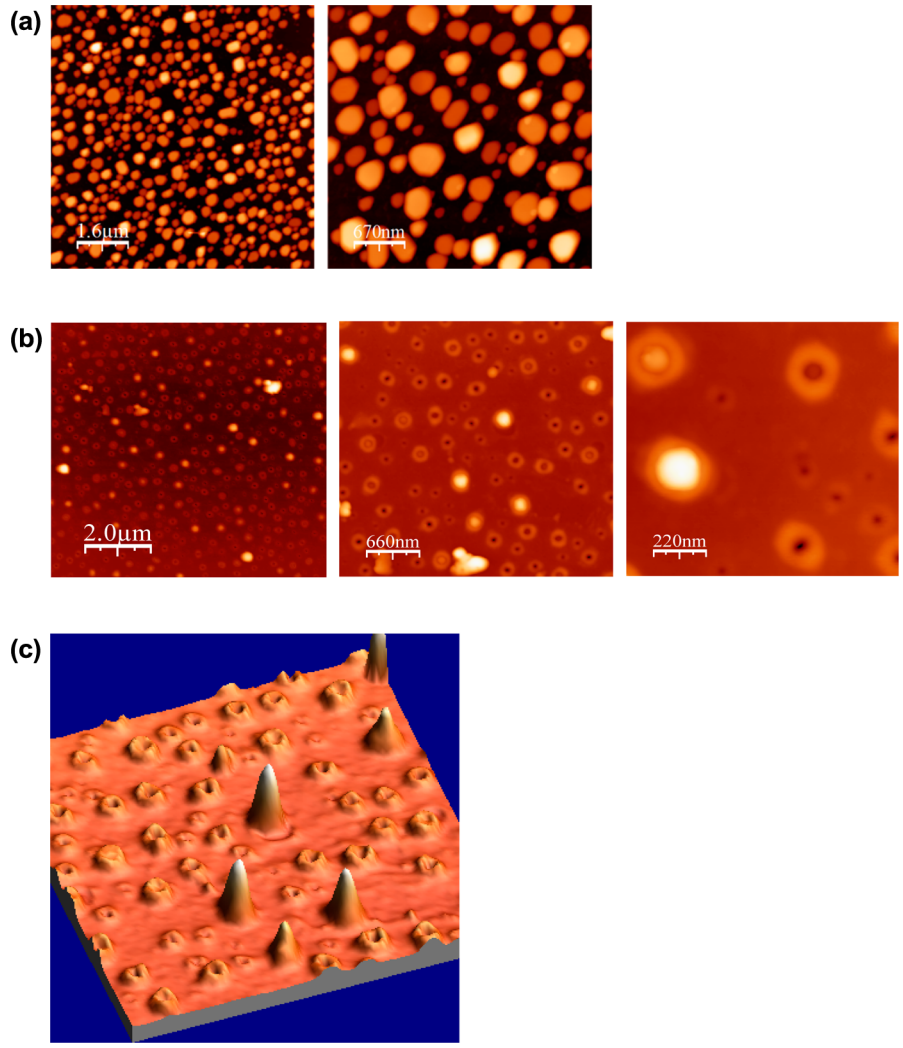

Figure 2. (a) AFM images of the sample that was annealed to 900 °C, showing the dewetting of the substrate to form Au nanoparticles. Image sizes are 8.0 × 8.0 μm for the left panel and 3.3 × 3.3 μm for the right panel. (b) AFM images of the sample which was annealed to 1100 °C, showing the formation of the unusual structures. Image sizes are 10 × 10 μm for the left panel, 3.3 × 3.3 μm for the middle, and 1.1 × 1.1 μm for the right panel. (c) 3D image of the surface annealed to 1100 °C (2.9 × 2.9 μm, maximum vertical height difference is 70 nm) showing both nanoparticles and raised rampart structures.

than at the lower temperature. If we go to higher magnification, however, we can discern that things are not so simple; the presence of particles, doughnut shapes, and pits of various sizes are seen dotted around the surface. In fact, when we examine the image at size 3.3 μm we can determine that the number of such features in the image is approximately the same as the particles in the image of Figure 2a. Figure 2c shows a three-dimensional (3D) representation of part of the surface, showing the presence of "volcano-like" structures; line scans of some of these structures are shown in Figure 4 of the Supporting Information, confirming these structural features. However, we must remember that AFM images of this sort exaggerate the *z*-direction because of the *z*-sensitivity of SPM techniques used to represent surface profiles at the ultrananoscale, so in reality these are more like central depressions in the surface surrounded by nanosized ramparts. In many cases there are raised regions inside the rampart, which equate with the presence of nanoparticles. The presence of gold nanoparticles is confirmed from the significant Au signal in the XPS spectrum after heating to 1100 °C (Figure 1). Note that this behavior is quite different from that observed on single-crystal alumina, which does not oxidize upon heating.[7,8]

To understand more fully the changes that have occurred on the surface and especially beneath the surface after annealing we employed SEM. This is carried out within the SEM/FIB system described above. Figure 3a shows an SEM image of the surface after annealing to 1100 °C. The difference between this and the AFM image is that more Au nanoparticles are evident (the bright features) because of the differences in the imaging mechanism, as described below. It is quite clear that the particles are generally in a "pit", and the silica surface is raised around the pit openings. Note that this image was taken with an angle between the electron beam and the surface of 36° with respect to the surface normal. This gives the image a somewhat strange appearance—that is, many particles appear to be in the side-wall of the pit. This is because the electron beam penetrates the pit-wall and can "see" the nanoparticle inside, giving a ghost image of the particle inside the hole. Note that the penetration depth (the inelastic mean free path) of the electron beam at these energies (3 keV) is ~7 nm (ref 10), and so particles can scatter the beam through parts of the wall of

dx.doi.org/10.1021/jp4074043 | J. Phys. Chem. C 2013, 117, 21577−21582

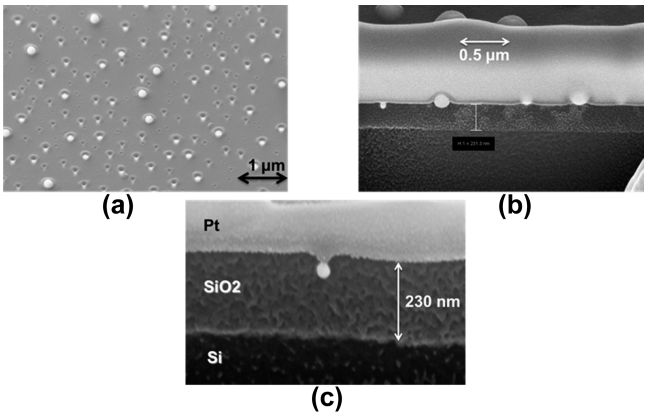

Figure 3. SEM images of the surface after annealing to 1100 °C. The top left image (a) is a standard one, whereas the top right image (b) is of a section of the surface cut from the sample using FIB and then raised above the original surface level for inspection. The lower image (c) is a magnification of part of the upper right image. In the latter, the two different layers of Pt described in the Experimental Section can be seen above the SiO_2 interface; these are deposited to aid in the fabrication process.

about this thickness and lower. These data indicate that there is neither a significant loss of Au from the surface, nor is sintering very evident. Therefore, option (iii) above applies, that is, there is some other cause for the reduction in Au signal in XPS after annealing to 1100 °C. The reduction in Au signal in the XPS between 900 and 1100 °C is likely to be due to the partial encapsulation of the Au particles

Figure 3b shows an SEM image of a surface cross-sectional profile. An FIB slicing cut was made at 90 degrees toward the surface, and the subsequent SEM imaging was taken at 36 degrees (toward the surface) allowing observation of the produced cross sections. Because the tilt compensation option of SmartSEM software was applied, there is no distortion of the cross-sectional images. Here we can get further insight into the processes taking place in the solid when annealing in air. We can see the thickness of the silica layer produced by oxidation at 1100 °C is ~230 nm, fitting in very well with the original data of Deal and Grove[13] for Si oxidation. This is much greater than the inelastic mean free path of the Si(2p) photoelectrons, explaining why no Si(0) signal is seen in Figure 1 after annealing to 1100 °C; this layer is evidently already thickening by 900 °C. It is clear from Figure 3b that the Au particles have become surrounded, to varying degrees, by SiO_2 and that this tends to grow around the particle, as illustrated in Figure 4. It appears, perhaps unsurprisingly, that smaller particles are more "buried" by SiO_2. However, also note that none of the particles in these images ever seem to be fully covered; a channel always remains to the outer surface. As impressive Figure 3b is, we must remember that it is a slice through a random arrangement of particles, that is, the cross sections of the particles we see are not likely to be through the exact center of the particles imaged.

Clearly, SiO_2 is growing on the original surface during oxidation as seen by the increase in the Si(2p) signal for Si(IV) at 103 eV. Note that the density of Si and SiO_2 are almost identical (2.33 and ~2.4 g cm^{-3}, respectively).[14] As a result of the oxidation, there is a volume expansion of 2.16 because the molecular density of SiO_2 is 2.3×10^{22} molecules/cm^3 and the atomic density of Si is 5.0×10^{22} atoms/cm^3; this growth is illustrated in Figure 4a. It is known that the oxidation of Si proceeds by diffusion of oxygen through the already-present

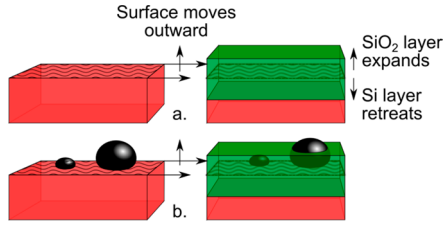

Figure 4. Schematic diagram of the oxidation of the Si crystal (shown in red) in the absence (a) and presence (b) of Au nanoparticles. In (a), as oxidation proceeds, the SiO_2 layer (shown in green) grows, and this must occur by net transport of Si outward from the original surface. Because the density of the two phases is similar, but the SiO_2 layer is about 50% as dense in Si as the Si crystal itself, the SiO_2 layer grows both out from the original surface plane and down from that layer into the bulk. When nanoparticles are present (b), here showing a smaller and a larger nanoparticle, then the tendency is for them to "float" on the growing SiO_2 and also to become encapsulated to different degrees. However, the real situation with the particles is even more complicated than this simple picture (see text and Figure 5 below).

oxide layer to the interface with the underlying Si where reaction takes place.[13,15] So we need to consider what happens to the Au particles when they are present on the surface as we oxidize the sample. A priori we might have imagined three scenarios: (1) the Au floats on top of the growing SiO_2 layer and remains entirely at the surface; (2) the Au remains anchored close to the original Si surface and becomes buried by growing SiO_2 (Figure 4b); (3) some mixture of these behaviors. At first, it might appear that possibility (1) is eliminated because of the evidence of the partial burial of the nanoparticles seen in AFM and SEM images. It would seem therefore that possibility (2) is the correct explanation. However, if that were the case, the particles should be located at approximately the original surface level, that is, about half-way through the oxide, because the particles were originally formed near this surface. It is apparent that the particles are much nearer to the surface of the oxide than that, yet they are at least partly buried in oxide. The amount of oxide under the Au particles is ~200 nm, whereas there is ~35 nm above the bottom of the particles. Thus, it appears that possibilty (3) is the case, though with behavior of (1) playing the dominant role.

Oxidation of the Si surface occurs at the interface between the two by the diffusion of oxygen through the oxide layer as described in the seminal paper by Deal and Grove in which they derived the widely accepted model for this process.[13] The oxide builds in a layer-by-layer fashion, from the interface, leading to contraction of the Si/SiO_2 interface inward and the expansion of the oxide surface outward, with each new oxide layer underpinning the ones formed before (above) it. Effectively, there is a net flux of Si upward toward the growing surface and net transport of oxygen inward below the original surface layer, as schematically illustrated in Figure 4. Thus, a Au nanoparticle remains anchored to the oxide layer to which it was originally attached, and so does indeed float on the growing layers, emanating from the Si interface underneath (Figure 4b). How then do we explain the fact that the particles become buried (at least partially)? We believe that this occurs because of simple blocking of oxygen adsorption onto the surface by the presence of the gold particles. It is known that gold does not readily oxidize with molecular oxygen because of the only weakly exothermic heat of formation of gold oxide[16,17] and its endergonic free energy of formation. This results in a normal growth rate of SiO_2 in the parts of the surface which are

dx.doi.org/10.1021/jp4074043 | J. Phys. Chem. C 2013, 117, 21577−21582

exposed to the gas phase, but a reduced growth directly underneath the particles themselves, as illustrated in Figure 5.

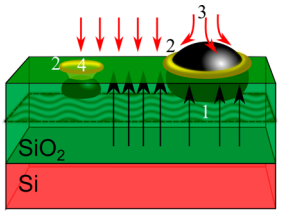

Figure 5. Schematic of the overgrowth mechanism of SiO_2 over the Au nanoparticles. Partial burial of the nanoparticles is due to the reduced supply of oxygen to the area underneath the nanoparticle (1). The "ramparts" (2) around the gold nanoparticles are due to the increased flux of oxygen at the edges of the particles by scattering from the gold (3). The SiO_2 layer appears not to wet the Au nanoparticles completely (4); the reasons for the holes being left in the surface above the small nanoparticles is discussed in the text.

Hence, the silica layer grows around and over the particles. However, the growth rate is only partly reduced, because the Au particles are lifted a considerable distance from the original surface position on the silica layer growing underneath them. This implies that there is significant lateral oxygen diffusion, so that it can access the regions underneath the particle, but that the flux there is reduced somewhat. It is likely that the effect is most marked at the beginning of oxidation (when there is little space for lateral diffusion of oxygen underneath the Au particles). The difference in oxidation rates between areas remote from the particle and directly under the particle probably diminishes as oxidation proceeds because the difference in vertical displacement of the top SiO_2 layers away from the Si interface and that same distance underneath the Au becomes small.

There are a couple questions that require further consideration. (i) Why are there raised areas of oxide at the periphery of the Au particles? (ii) Why are there holes above even the smallest Au particles?

Regarding (i), it is likely due to the process illustrated in Figure 5, that is, the net flux of oxygen from the gas phase in the immediate vicinity of the Au particle is a little higher than that elsewhere because of an enhanced scattering flux from the Au particles in that area. In other words, the effective pressure adjacent to the particles is higher than that further away from them. This process is also illustrated in Figure 5. There also appears to be a negative interaction between the SiO_2 and the Au, indicated by the acute wetting angle, which leads to a depletion of SiO_2 immediately next to the particle. Therefore, additional oxidized material is built up slightly further from the particle, leading to the distinctive doughnut shapes seen in the AFM images of Figure 2 and SEM images of Figure 3.

Question (ii) above is rather more difficult to understand. Complete burial of the particles does not occur, as seen in the SEM and AFM images. On the contrary, there is a lot of evidence of the "ring and ditch" structures with Au particles present in the middle of holes in the surface, which is especially evident in the SEM images. So why is this hole always left? It could be related to the nonwettability of the Au surface with respect to the silica mentioned above. Alternatively, it may simply be that the silica growth occurs generally in a linear manner with the growth mainly in the vertical direction, so a hole is left where this cannot occur. Again, this may be especially important in the initial stages of growth in which the oxidation is driven by large potential difference gradients perpendicular to the surface, as described originally by Cabrera and Mott,[14] which slow the process considerably after that stage, leaving the particle in a hole. At present we cannot say which of these processes is dominant.

These findings would benefit from an extension to other metal nanoparticle−oxide growth systems. We believe it will be discovered for a number of other metal-oxide−semiconductor junctions for which the semiconductor can be oxidized (e.g., Pt−GaAs). These phenomena are of considerable relevance to the semiconductor fabrication industry, especially at a time when devices, and especially metal contacts and wires, are becoming ever smaller in the nanosize range. Si oxidation processes occur around such structures. The processes described here may represent an opportunity for the controlled stabilization of nanostructures of this kind. Even for catalysis, where the nanoparticles used are generally much smaller than those discussed here, such partial encapsulation could represent a way of stabilizing small particles against sintering.

■ ASSOCIATED CONTENT

Supporting Information

AFM images with line scans over particles and particle size distributions, linking with the figures and discussions in the main text. This material is available free of charge via the Internet at http://pubs.acs.org.

■ AUTHOR INFORMATION

Present Addresses

[‖]J.J.C.: BP, Chertsey Road, Sunbury-on-Thames, Middlesex TW16 7LN, U.K.

[⊥]S.D. and D.-T.P.: School of Mechanical Engineering, University of Birmingham, Birmingham B15 2TT, U.K.

Notes

The authors declare no competing financial interest.

■ ACKNOWLEDGMENTS

This work was partly funded by EPSRC and Cardiff University.

■ REFERENCES

(1) Haruta, M.; Kobayashi, T.; Sano, H.; Yamada, N. Novel Gold Catalysts for the Oxidation of Carbon Monoxide at a Temperature Far Below 0 °C. *Chem. Lett.* **1987**, 405−407.

(2) Haruta, M.; Yamada, N.; Kobayashi, T.; Iijima, S. Gold Catalysts Prepared by Coprecipitation for Low-Temperature Oxidation of Hydrogen and of Carbon Monoxide. *J. Catal.* **1989**, *115*, 301−311.

(3) Landon, P.; Collier, P. J.; Papworth, A. J.; Kiely, C. J.; Hutchings, G. J. Direct Formation of Hydrogen Peroxide from H_2/O_2 Using a Gold Catalyst. *Chem. Commun.* **2002**, 2058−2059.

(4) Hughes, M. D.; Xu, Y.-J.; Jenkins, P.; McMorn, P.; Landon, P.; Enache, D. I.; Carley, A. F.; Attard, G. A.; Hutchings, G. J.; King, F.; et al. Tunable Gold Catalysts for Selective Hydrocarbon Oxidation Under Mild Conditions. *Nature* **2005**, *437*, 1132−1135.

(5) Balamurugan, S.; Mayer, K M; Lee, S.; Soper, S A; Hafner, J. H; Spivak, D. A. Nanostructure Shape Effects on Response of Plasmonic Aptamer Sensors. *J. Mol. Recognit.* **2013**, *26*, 402−407.

(6) Ruemmele, J. A.; Hall, W. P.; Ruvuna, L. K.; Van Duyne, R. P. A Localized Surface Plasmon Resonance Imaging Instrument for Multiplexed Biosensing. *Anal. Chem.* **2013**, *85*, 4560−4566.

(7) Bowker, M.; Carley, A. F.; Davies, P. R.; Morgan, D.; Crouch, J.; Lalev, G.; Dimov, S.; Pham, D.-T. Effects of the Nanostructuring of Gold Films upon Their Thermal Stability. *ACS Nano* **2010**, *4*, 2228−2232.

(8) Bowker, M.; Broughton, M.; Carley, A. F.; Davies, P. R.; Morgan, D. J.; Crouch, J.; Lalev, G. M.; Dimov, S.; Pham, D.-T. Influence of Thermal Treatment on Nanostructured Gold Model Catalysts. *Langmuir* **2010**, *26*, 16261−16266.
(9) WSxM Program. http://www.nanotec.es/products/wsxm/index.php.
(10) Werner, W. Electron Transport in Solids for Quantitative Surface Analysis. *Surf. Interface Anal.* **2001**, *31*, 141−76.
(11) Cumpson, R. The Thickogram: A Method for Easy Film Thickness Measurement in XPS. *Surf. Interface Anal.* **2000**, *29*, 403−6.
(12) Morita, M.; Ohmi, T.; Hasegawa, E.; Kawakami, M.; Ohwada, M. Growth of Native Oxide on a Silicon Surface. *J. Appl. Phys.* **1990**, *68*, 1272−81.
(13) Deal, E.; Grove, A. S. General Relationship for the Thermal Oxidation of Silicon. *J. Appl. Phys.* **1965**, *36*, 3770−8.
(14) *Handbook of Chemistry and Physics*, 82nd ed.; Lide, D. R., Ed. CRC Press: Boca Raton, FL, 2001; pp 4−81.
(15) Massoud, H. Z.; Plummer, J. D.; Irene, E. A. Silicon Dry Oxidation Kinetics at Low Temperature in the Nanometric Range. *J. Electrochem. Soc.* **1985**, *132*, 2685−2695.
(16) Ashcroft, S.; Schwartzmann, E. Standard Enthalpy of Formation of Crystalline Au(III) Oxide. *J. Chem. Soc., Faraday Trans. 1* **1972**, *68*, 1360−1361.
(17) Shi, H.; Asahi, R.; Stampfl, R. Properties of the Gold Oxides Au_2O_3 and Au_2O: First Principles Investigation. C. *Phys. Rev. B* **2007**, *75* (205125), 1−10.
(18) Cabrera, N.; Mott, N. F. Theory of the Oxidation of Metals. *Rep. Prog. Phys.* **1948**, *12*, 163−184.